

# Primary electron energy dependent flashover in surface polarity on Au films

M. Catalfano,<sup>1</sup> A. Kanjilal,<sup>1,2</sup> A. Al-Ajlony,<sup>1</sup> S. S. Harilal,<sup>1</sup> and A. Hassanein<sup>1</sup>

<sup>1</sup>Center for Materials Under Extreme Environment, School of Nuclear Engineering Purdue University, West Lafayette, Indiana 47907, USA

<sup>2</sup>Department of Physics, School of Natural Sciences, Shiv Nadar University, Uttar Pradesh 203207, India

(Received 19 December 2012; accepted 12 April 2013; published online 1 May 2013)

Primary electron energy ( $E_p$ ) dependent change in target current was studied on a grounded Au film in the range of 40 to 3500 eV. The current jumped suddenly from a negative to a positive value at  $\sim 650$  eV with increasing  $E_p$ , while it disappeared in reverse sweep and with increasing substrate temperature. Detailed analysis suggests that  $E_p$  dependent surface charging plays a pivotal role in flashover. Prior to critical  $E_p$  in the forward sweep, a gradual shift of a double peak-like structure towards high kinetic energy region in the secondary electron spectra also confirms surface charging effect. © 2013 AIP Publishing LLC. [<http://dx.doi.org/10.1063/1.4803484>]

## I. INTRODUCTION

Incident electron-induced charging of insulators in vacuum can lead to multipacting, errors in lithography, and surface flashover. So far, it is known that electrons fired at a dielectric target in vacuum either become caught in traps,<sup>1</sup> or escape from the irradiated volume to the ground via sample holder, or eject secondary and backscattered electrons.<sup>2</sup> When electrons are trapped, negative charges are accumulated in the bulk, while positive charges are formed on the surface through the ejection of secondary and backscattered electrons.<sup>2,3</sup> This difference in charge creates an electric field, which can sometimes be strong enough to de-trap the embedded electrons.<sup>4</sup> This so called “space charge” can be affected by many variables such as energy of the injected electrons,<sup>5</sup> time,<sup>6</sup> temperature,<sup>7</sup> defect concentration,<sup>8</sup> sample thickness,<sup>9</sup> and atmosphere.<sup>10</sup> The space charge is directly related to the amount of secondary electrons escaping per incident electron, also known as the secondary electron yield (SEY). When plotted against energy, it typically has a bell-like shape to which has been assigned a universal formula.<sup>11</sup> However, there are several unanswered questions that are impeding the advancement of many important applications under electron bombardment, including spacecraft charging,<sup>12</sup> e-beam lithography,<sup>13</sup> and electron microscopy.<sup>4</sup>

Generally, the SEY reaches a value of 1 at two critical energies, usually labeled as  $E_1$  and  $E_2$  ( $E_2 > E_1$ ).<sup>2</sup> Below  $E_1$  and above  $E_2$ , the surface potential is negative. However, between these two values it is positive, due to the holes left behind while electrons are escaping from the material. The  $E_2$  value can often shift as a function of excess charge.<sup>2</sup> When examining the SEY of various elements, there is a great deal of discrepancy in the experimental data.<sup>14</sup> Many of these discrepancies were due to the presence or absence of oxide growth and carbon contamination on the surface of various elements,<sup>15</sup> causing an increase in the SEY. Given the right circumstances, a sudden change in polarity can occur in insulating materials, leading to either surface flashover<sup>16</sup> or dielectric breakdown.<sup>17</sup> This can be due to electron-electron cascades, governed by defects in the material and adsorbed gas on the surface.<sup>18</sup> Polarons in the

dielectric material were also considered to be trapped in the sites of low susceptibility, while the surface breakdown (flashover) was modeled in the light of both charge de-trapping and sudden relaxation of energy of polarization.<sup>16</sup> If the electron-induced charge buildup and/or the scattering of charges in defect sites can play a decisive role in insulators, what will be the impact on the emitted secondary electrons from the sample surface? In fact, the knowledge of charge relaxation in insulators under electron irradiation is crucial for several applications, especially when a thin layer of conductive material is needed for obtaining the surface morphology of an insulating material in scanning electron microscopy.<sup>6</sup> Now the question is what will happen if such a metallic film on an insulating layer has been exposed to a continuous beam of electrons with increasing energy? Will the probability of polarity shift still exist if the electron penetration depth is much smaller than the thickness of the metallic film?

In this paper, we investigate the electrical property of Au film grown on a quartz substrate. In particular, we monitor the change in target current with increasing and decreasing primary electron energy ( $E_p$ ) in the range of 40 to 3500 eV, called *forward* and *reverse* sweeps, respectively, in an ultrahigh vacuum (UHV) chamber. We have seen a sudden change in polarity at 650 eV in the forward sweep, whereas such intriguing phenomenon disappears in reverse sweep and with increasing substrate temperature. Chemically inert Au surface is chosen to exclude the effect of surface contamination. We have also monitored the corresponding secondary electron emission (SEE) spectra to understand the charging behavior as a function of  $E_p$ , especially the relative contribution of the surface and bulk charging properties and the role of defects.

## II. EXPERIMENT

All experiments were performed in the IMPACT facility<sup>19</sup> at the Center for Materials Under Extreme Environments (CMUXE) at Purdue University. The schematic of the experimental setup used for the present study is given in Fig. 1. Here a 300 nm thick Au layer grown on a

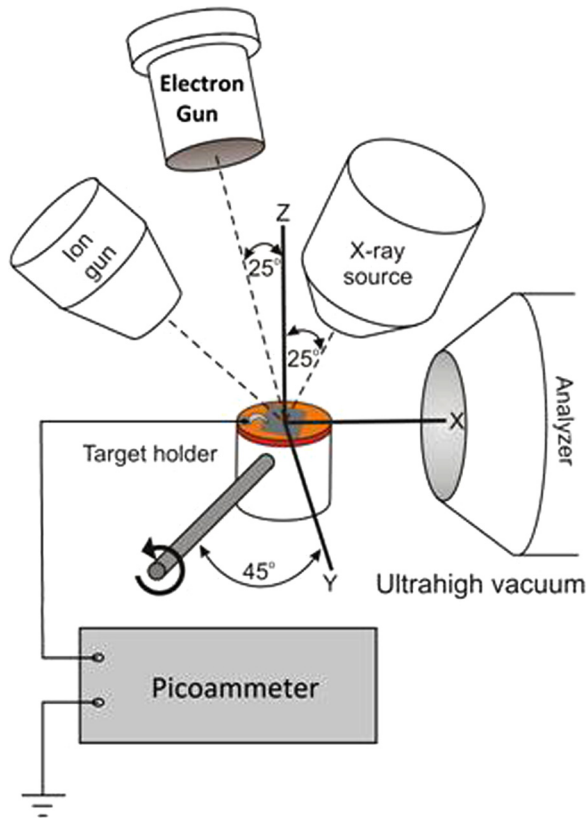


FIG. 1. Schematic view of the sample holder in IMPACT chamber. The  $1 \times 1 \text{ cm}^2$  sample is held on by a metallic clamp, which is grounded from the body of the copper target holder through the picoammeter. Sputtering was performed at a  $0^\circ$  rotation while XPS and SEE were performed at  $45^\circ$  from the Z axis.

$1 \times 1 \text{ cm}^2$  quartz substrate was bombarded by a continuous electron beam with a SPECS EQ-22 electron gun in the UHV chamber (base pressure of  $\sim 3 \times 10^{-9}$  Torr). The electron gun emission current was kept constant throughout the experiment at  $1 \mu\text{A}$ , while the Wehnelt voltage was set at 2 V. The maximum electron flux reaching the sample was  $\sim 5 \times 10^{11}$  electrons/ $\text{cm}^2\text{s}$ . Each sample was held on a grounded target holder using a metallic clamp, at the very edge of the surface (see Fig. 1). Prior to electron exposure with  $E_p$  in the range of 40 to 3500 eV, the Au surface was sputter cleaned by 1 keV  $\text{Ar}^+$ . The surface contamination level was verified by using x-ray photoelectron spectroscopy (XPS), with an Al- $K_\alpha$  source ( $h\nu = 1486.65 \text{ eV}$ ), while emitted photoelectrons were collected at  $45^\circ$  from the sample surface and analyzed by a SPECS Phoibos-100 hemispherical electron analyzer (HEA) with an energy resolution of 0.85 eV. For XPS, the binding energy scale with respect to the measured kinetic energy (KE) was calibrated using silver Fermi edge. Emitted electrons were analyzed by the HEA, where it took about 2 min 45 s to record a SEE spectrum with a pass-energy of 4 eV. The primary electron energy was only changed at the end of each scan. The target current was measured in series with a grounded Keithley-6485 picoammeter, with a rise time of 8 ms. The current measurements were taken at the end of each SEE scan. The error in the measured current, through several measurements, was found to be about  $\pm 7\%$ .

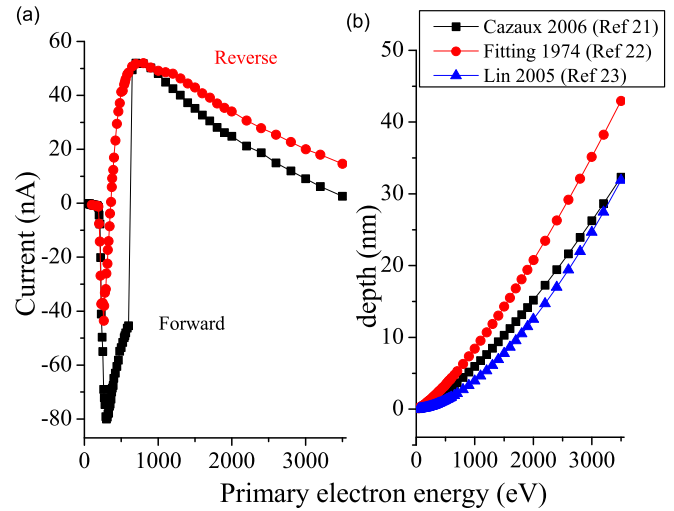


FIG. 2. (a) Current profiles of freshly sputtered Au film grown on quartz, taken with forward (from 40 to 3500 eV) and reverse (from 3500 to 40 eV) sweeps. (b) Calculated penetration depth of injected electrons on Au, assuming constant energy loss with material where the constants taken from labeled references.

### III. RESULTS AND DISCUSSION

The forward and reverse current profiles of the Au layer as a function of  $E_p$  in the range of 40 to 3500 eV are displayed in Fig. 2(a). As can be seen, a sudden change in polarity (flashover) has been recorded at 650 eV during the forward sweep. However, the flashover is absent in the reverse sweep. We should note here that the sample was sputter cleaned too by 1 keV  $\text{Ar}^+$  before taking the reverse sweep. The recorded current is associated with the leakage current directly from the target material and the image displacement current from the metallic target holder.<sup>20</sup> However, the leakage current should be dominant because we took the current measurements in a steady state condition.<sup>20</sup> In order to understand the observed flashover in the forward sweep, the experiment was also performed without the metallic clamp. Here, we did not find any flashover, indicating that the sudden change in surface polarity is strongly related to the leakage current from the top Au layer. All the recorded data were found to be repeatable.

Because the metal-dielectric interface is about 300 nm under the Au surface, it would be beneficial to know the penetration depth of the injected electrons into the Au layer. The penetration depth of electrons was modeled using the assumption of constant energy loss,

$$R = CE_p^n, \quad (1)$$

where  $R$  is the penetration depth in nanometers,  $E_p$  in keV,  $n$  is a fitting constant, and  $C$  depends on the material density. The model was checked for three different constants,<sup>21–23</sup> where the  $E_p$  dependent calculated penetration depths are exhibited in Fig. 2(b). As discerned, the maximum penetration depth of the 3500 eV electrons is about 40 nm from the Au surface. This was also confirmed by using the CASINO Monte Carlo electron code.<sup>24</sup> This implies that the Au/quartz interface does not have a direct effect on the flashover. To test whether or not the interface was the deciding factor,

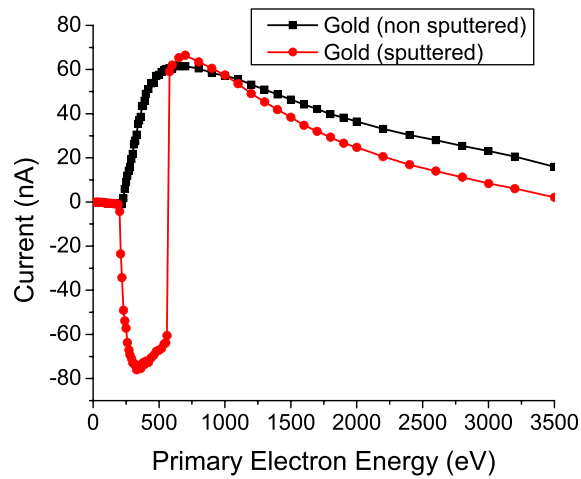


FIG. 3. Current profiles of freshly sputtered Au film grown on quartz as a function of  $E_p$  in forward (from 40 to 3500 eV) sweep, compared to a sample which has not been sputter cleaned.

similar experiments were performed on graphite and silicon substrates. Interestingly, the flashover effect was also seen in both samples, but it only occurred after sputter cleaning the surface by 1 keV  $\text{Ar}^+$  as the one observed for Au in Fig. 3. Although the flashover curve seems to be universal in the forward sweep, the critical  $E_p$  and the curve shape were different in each material. It is clear that there is some other mechanism behind flashover. Is the observed flashover then controlled by the atomic number,  $Z$ , of the material? A recent model by Cazaux<sup>25</sup> which takes the radial dispersion of electrons into account based on the atomic mass uses the factor,

$$k = \frac{z_c}{R} = 0.5e^{-0.022(Z)}, \quad (2)$$

where  $z_c$  is the most probable energy dissipation depth, and  $\langle Z \rangle$  is the mean atomic number of the material. The  $k$  describes electron cascades confined in an elliptical area under the surface. According to the equation, a low  $Z$  material, such as carbon, should have a long major axis extending into the depth, while a high  $Z$  material like Au will be spread out along the surface in a semi-circle. In other words, the  $Z$  dependence indicates that a low atomic number material will have an electron cascade that extends deeper into the material than that of a high  $Z$  material such as gold. As the flashover was found on both carbon and Si (see Fig. 4), we can discard the contribution of  $Z$ .

Since the  $\text{Ar}^+$  sputter cleaning was found to be indispensable for observing the flashover (Fig. 3), it is quite possible that the surface defects and/or roughness can take part in trapping charges needed to initiate flashover. It has earlier been shown that the flashover of dielectrics is directly related to the roughness of the surface: the lower the roughness, the higher the breakdown potential of the material—so less chance of getting flashover.<sup>26</sup> Since the 1 keV  $\text{Ar}^+$  ions are sufficient enough to damage the surface crystalline structure, we believe that the localized change in the surface chemical property in the ion beam induced defects can play a significant role to trap electrons. Indeed, the active defect centers, especially vacancies can react locally with oxygen and/or

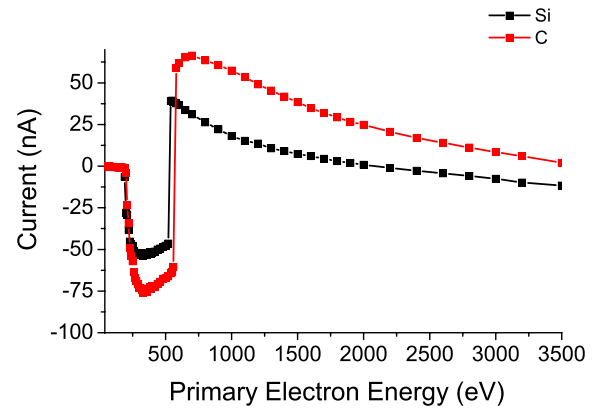


FIG. 4. Current profiles of freshly sputtered C and Si as a function of  $E_p$  in forward sweep (from 40 to 3500 eV).

carbon atoms via electron-induced dissociation of residual hydrocarbons and water molecules. More careful analysis of the surface is therefore needed for detailed understanding (will be discussed in the following).

Why does the flashover not occur in the reverse sweep [Fig. 2(a)]? This can be explained in the following way: because the scan starts at the maximum  $E_p$ , most of the incoming electrons can penetrate deep inside the bulk. When the injected electrons travel through the bulk material, they can encounter several atomic sites. Because of the collision with the orbital electrons, a large number of secondary electrons can be produced. These freshly created secondary electrons can be multiplied further when they move towards the surface in cascades, and thereby give a large SEY. This in turn creates a large positive potential at the surface. As the  $E_p$  was reduced gradually, electrons that could have been trapped in the defect centers are instead attracted to the positive surface. The negative charge layer in the bulk can also repel the low energy electron towards the surface, which as a result can initiate rapid recombination of electrons to the holes near the surface and lower the landing energy of incoming electrons.<sup>2</sup> Soon after crossing the critical  $E_p$  (650 eV for Au), electron trapping effect becomes superior over hole generation near the surface, showing a slight dip in the current profile [Fig. 2(a)]. However, the electron trapping is not as large as in the case of the forward sweep because of the existence of a large number of holes, and therefore no flashover occurs.

Because of the compatibility to Fig. 2(a), a surface sensitive SEE spectroscopy technique was employed in both forward and reverse sweeps in order to follow the change in surface property. Here the SEE spectrum was recorded for every measured point in Fig. 2(a). The secondary electron distribution with KE was measured up to 60 eV, so that each spectrum can take into account both pure secondary and some backscattered electrons.

Typical forward sweep SEE spectra of the sputter cleaned Au film were displayed in Fig. 5, where each scan took  $\sim 2$  min 45 s. We show only for  $E_p$  in the range of 40 to 1000 eV for better projection of the impact of surface flashover. Each spectrum is characterized by two main features: (i) inelastically scattered electrons and (ii) pure secondary

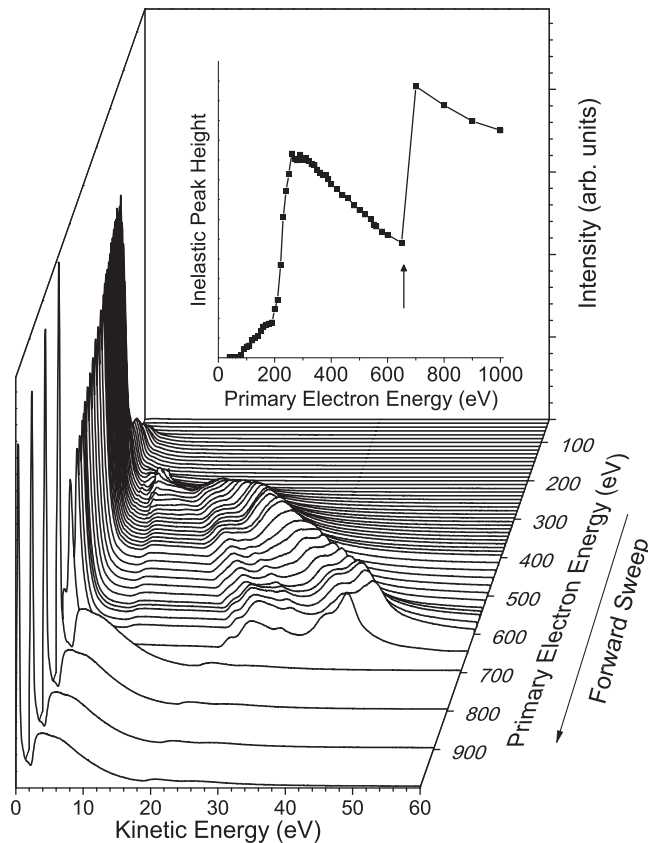


FIG. 5. SEE spectra of Au film in forward sweep up to 1000 eV for clarity, where each spectrum takes 2 min 45 s. The inset shows the variation of the inelastic peak intensity with increasing  $E_p$ , while  $\uparrow$  indicates the flashover point.

electrons. The change in the inelastic peak intensity with respect to  $E_p$  is exhibited in the inset of Fig. 5. It shows that the peak intensity increases gradually up to  $\sim 200$  eV, followed by a sharp rise in intensity up to 260 eV before attaining the flashover at 650 eV with a monotonic decrease in intensity. The intensity again jumps to its highest value at 700 eV, followed by a decrease in intensity with further increase in  $E_p$ . Close inspection reveals a tail beside the inelastic peak extending towards high KE region below 150 eV.

Following the slow disappearance of the tail above 150 eV, a weak but clear secondary electron peak originating at  $\sim 4.3$  eV KE can be observed when  $E_p$  was increased to 200 eV. The 4.3 eV peak was found to intensify and shift to  $\sim 10$  eV prior to become weaker with further increase in  $E_p$  above 230 eV, provided a new peak was found to evolve at  $\sim 15$  eV KE at 230 eV. Interestingly, the peak at  $\sim 15$  eV KE again split into two with increasing  $E_p$  above 260 eV, and continuously moves towards high KE region. The final positions of those peaks right before the flashover were 27.8 eV and 45.1 eV KE, while some fine structures can also be resolved (see Fig. 5). As the flashover occurs at 650 eV, the peaks were found moving rapidly to the lower energy side with reduced intensity, accompanied by a sudden appearance of a strong peak at  $\sim 4.3$  eV KE from 700 eV onward.

Looking to Fig. 5, slow movement of the secondary electron peaks towards high KE region with increasing  $E_p$  up

to 650 eV can be assigned to surface charging by free electrons.<sup>2</sup> Due to the positive charging of the Au surface above 650 eV, it seems that the secondary electrons are involved in partial neutralization of the surface potential by recombining with holes. Low KE electrons are known to be associated with surface and bulk plasmons, while low energy incident electrons are favorable for surface plasmon excitation.<sup>27</sup> Note that the plasmons excited by electron energy losses decay via creation of electron-hole pairs, acting as a source of SEs.<sup>27</sup> The depth of the volume plasmon excitation which is expected to be comparable to the escape depth of SEs is associated with the volume band structure. On the other hand, the surface plasmon decay is mainly related to the surface band structure. Moreover, the cascades of higher-order secondaries for the surface and bulk in plasmon decay differ in magnitude and thus cause different peak broadening.<sup>27</sup> Due to close proximity of the surface and bulk plasmon loss, one can, however, expect overlapping of these peaks and so to see a broad band at energies corresponding to the surface and volume plasmon energies in a SEE spectrum as the one demonstrated both experimentally and theoretically for Al(100) substrates with 100 eV electron bombardment.<sup>27</sup> Although the appearance of the secondary electron peak at  $\sim 15$  eV and above is not clear at this moment, we can assign the 4.3 eV KE peak as an outcome of the decay of long wavelength surface and volume plasmons via near vertical interband transition.<sup>27,28</sup> A similar peak has also been observed previously in polycrystalline metals,<sup>29</sup> while Joy found the Au peak to reside at 5 eV.<sup>30</sup> Interestingly, the appearance of a weak shoulder related to the volume plasmon loss (at  $\sim 10$  eV) has been reported adjacent to the relatively strong surface plasmon peak (at  $\sim 5$  eV) in a typical SEE spectrum from a 100 eV electron bombarded Al surface.<sup>27</sup> Therefore, the onset of the continuous shift of the 4.3 eV peak towards 10 eV KE right before the evolution of a new peak at  $\sim 15$  eV with increasing  $E_p$  up to 230 eV (Fig. 5) is possibly associated with the increasing contribution of the SE yield due to volume plasmon decay over surface plasmon decay with increasing electron trapping near the surface (discussed above). On the other side, continuous increase in inelastic peak intensity up to 230 eV  $E_p$  is most likely related to the increase in interaction of surface atoms with injected electrons, while the gradual decrease in inelastic peak intensity above 230 eV  $E_p$  up to the flashover, and even after the flashover seems to be associated with the recombination of inelastically scattered electrons with the holes which were left behind on the surface due to emission of SEs with KE above 15 eV (inset, Fig. 5). The contamination on the Au surface was found to be negligible after taking the SEE scans by XPS, implying that the flashover is not related to the adsorbed water or hydrocarbons on the surface. Therefore, we can rule out the Auger de-excitation process<sup>31</sup> on Au.

The origin of the SE peak near 15 eV for  $E_p$  above 230 eV (inset, Fig. 5) can be due to the increase in electron trapping near the surface, forcing the secondary electrons to gain extra energy upon escape due to Coulomb repulsion. In other words, the electrons buried just beneath the surface at low  $E_p$  ( $< E_1$ ) may act as a barrier, causing incoming electrons above it to reduce their landing energy, and cause them

to scatter from the surface with higher energy due to the repulsive force. Generally this effect was seen above  $E_2$ ,<sup>2</sup> but in this case, it also occurs before  $E_1$  where the surface is also negative. Meanwhile, electrons below the negative surface layer are directed further into the bulk and ultimately towards the interface, as proven by using the non-conducting clamp (stated above). With increasing  $E_p$ , the formation of an electron barrier due to trapping electrons near the surface will be more pronounced, and thus possibly allowing more inter-band transitions,<sup>28</sup> needed for explaining the observed fine structures in the pure secondary electron region (Fig. 5). This is also why the electrons are accelerated with progressively higher KE with increasing  $E_p$ , as indeed the peaks constantly gain energy. When the flashover occurs, according to the model given in Ref. 16, we can explain the observed fact in the light of escape of trapped electrons at once along the surface to the ground via the clamp. This as a result increases inelastically scattered electrons as shown by the sudden rise in peak intensity in Fig. 5 (inset). Finally, the escaped electrons leave behind a temporary positive charge which recombines with internal cascade electrons as  $E_p$  is further increased. Moreover, the gradual reduction of the plasmon peak intensity above flashover  $E_p$  can be assigned to the increasing loss of emitted SEs due to electron-hole recombination at the surface (Fig. 5).

As expected, when performing a reverse sweep [see Fig. 2(a)], we did not see any extra secondary electron peaks,

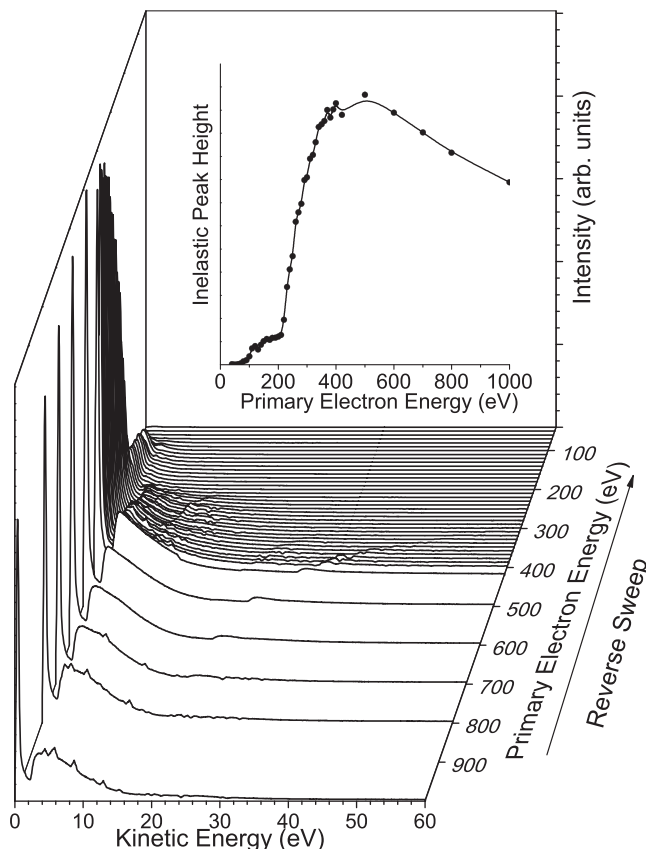


FIG. 6. SEE spectra of Au film in reverse sweep, showing from 1000 eV for better projection, where each spectrum takes 2 min 45 s. The inset shows the change in the inelastic peak intensity with decreasing  $E_p$ .

except for the 4.3 eV peak as the one seen after the flashover in the forward sweep (see Fig. 5). We found a similar phenomenon when we increased the substrate temperature to 100 °C (Fig. 6), where the corresponding current profile as a function of  $E_p$  is almost similar to the case of reverse sweep [Fig. 2(a)]. In both the reverse and high temperature cases, there was an increase in inelastic scattering up to about 500 eV, followed by a gradual decrease in intensity (Fig. 6). Compared to the discussion for Fig. 2(a), the initial increase in inelastic peak intensity can be explained in the framework of surface negative charge induced repulsion of incident electrons, whereas the decrease in intensity can be explained in terms of electron-hole recombination near the surface with increasing  $E_p$ .

Now the question comes, at high temperature, why do we not see any flashover? Thermal phonons often generated in a material with increasing temperature and can take part in interaction with electrons. Since the increased temperature on metals decreases the conductivity due to electron-phonon interaction,<sup>32</sup> we can expect a similar phenomenon on Au film at 100 °C. It seems that the secondary electrons are randomly scattered inside the Au film when interacting with thermal phonons, and thus cannot allow the electrons to be trapped. Hence, it is not possible for the electrons to escape suddenly at 100 °C—a prerequisite for the flashover.

#### IV. CONCLUSION

We have shown a sudden change in polarity (flashover) with increasing incident electron energy  $E_p$  in the range of 40 to 3500 eV on a grounded Au film. The flashover was only seen in forward sweep, but not in the reverse sweep. As the 300 nm thick Au film was grown on a quartz substrate, the target current was examined by replacing the metallic clamp with a bad conductor at the edge of Au surface. The absence of flashover in the later case implies that the flashover is a surface phenomenon rather than bulk. This is also supported by the calculated maximum penetration depth in Au for electrons in the range of 40 nm for 3500 eV. Further, SEE spectroscopy also confirms strong contribution of the surface on the observed flashover in forward sweep, showing the negative surface charging mediated continuous shift in spectra and change in spectral shape up to the flashover point at  $E_p = 650$  eV. However, this effect was not observed in reverse sweep, and also for forward sweep at 100 °C substrate temperature, showing only a single peak at  $\sim 4.3$  eV KE for  $E_p$  higher than 230 eV. The disappearance of the flashover has been discussed in terms of screening of secondary electrons through recombination with holes near the surface in reverse sweep, while the temperature induced electron-phonon interaction seems to control the overall mechanism.

#### ACKNOWLEDGMENTS

This work was partially supported by College of Engineering, Purdue University and the US Department of Energy.

- <sup>1</sup>H. S. Guo, W. Maus-Friedrichs, and V. Kempter, *Surf. Interface Anal.* **25**, 390 (1997).
- <sup>2</sup>J. Cazaux, *J. Electron Spectrosc. Relat. Phenom.* **176**, 58 (2010).
- <sup>3</sup>J. R. Dennison, C. D. Thomson, and A. M. Sim, *Proc. IEEE* **2**, 967 (2004).
- <sup>4</sup>J. Cazaux, *Scanning* **26**, 181 (2004).
- <sup>5</sup>J. Cazaux, *J. Appl. Phys.* **59**, 1418 (1986).
- <sup>6</sup>S. Fakhfakh, O. Jbara, and Z. Fakhfakh, *Phys. Procedia* **2**, 1391 (2009).
- <sup>7</sup>J. P. Vigouroux, J. P. Duraud, A. Lemoel, C. Legressus, and D. L. Griscom, *J. Appl. Phys.* **57**, 5139 (1985).
- <sup>8</sup>W. Q. Li and H. B. Zhang, *Micron* **41**, 416 (2010).
- <sup>9</sup>W. Q. Li and H. B. Zhang, *Appl. Surf. Sci.* **256**, 3482 (2010).
- <sup>10</sup>H. S. Guo, W. Maus-Friedrichs, V. Kempter, and Y. Ji, *J. Vac. Sci. Technol. A* **21**, 1009 (2003).
- <sup>11</sup>R. Mayer and A. Weiss, *Phys. Rev. B* **38**, 11927 (1988).
- <sup>12</sup>N. Balcon, D. Payan, M. Belhaj, T. Tondou, and V. Inguibert, *IEEE Trans. Plasma Sci.* **40**, 282 (2012).
- <sup>13</sup>W. Liu, J. Ingino, and R. F. Pease, *J. Vac. Sci. Technol. B* **13**, 1979 (1995).
- <sup>14</sup>C. G. H. Walker, M. M. El-Gomati, A. M. D. Assa'd, and M. Zadrazil, *Scanning* **30**, 365 (2008).
- <sup>15</sup>J. Cazaux, *J. Appl. Phys.* **110**, 024906 (2011).
- <sup>16</sup>G. Blaise and C. Legressus, *J. Appl. Phys.* **69**, 6334 (1991).
- <sup>17</sup>C. Legressus and G. Blaise, *IEEE Trans. Electrical Insulation* **27**, 472 (1992).
- <sup>18</sup>C. Legressus, F. Valin, M. Henriot, M. Gautier, J. P. Duraud, T. S. Sudarshan, R. G. Bommakanti, and G. Blaise, *J. Appl. Phys.* **69**, 6325 (1991).
- <sup>19</sup>A. Kanjilal, M. Catalfano, S. S. Harilal, A. Hassanein, and B. Rice, *J. Vac. Sci. Technol. A* **30**, 041401 (2012).
- <sup>20</sup>M. Belhaj, T. Tondou, V. Inguibert, B. Elsaifi, S. Fakhfakh, and O. Jbara, *Nucl. Instrum. Methods B* **270**, 120 (2012).
- <sup>21</sup>J. Cazaux, *Nucl. Instrum. Methods B* **244**, 307 (2006).
- <sup>22</sup>H. J. Fitting, *Phys. Status Solidi A* **26**, 525 (1974).
- <sup>23</sup>Y. H. Lin and D. C. Joy, *Surf. Interface Anal.* **37**, 895 (2005).
- <sup>24</sup>CASINO Monte Carlo electron code <http://www.gel.usherbrooke.ca/casino/download.html>.
- <sup>25</sup>J. Cazaux, *J. Phys. D* **38**, 2433 (2005).
- <sup>26</sup>O. Yamamoto, T. Takuma, M. Fukuda, S. Nagata, and T. Sonoda, *IEEE Trans. Dielectrics Electrical Insulation* **10**, 550 (2003).
- <sup>27</sup>W. S. M. Werner, A. Ruocco, F. Offi, S. Iacobucci, W. Smekal, H. Winter, and G. Stefani, *Phys. Rev. B* **78**, 233403 (2008).
- <sup>28</sup>M. S. Chung and T. E. Everhart, *Phys. Rev. B* **15**, 4699 (1977).
- <sup>29</sup>J. J. Lawton, A. Pulisciano, and R. E. Palmer, *J. Phys.-Condens. Matter* **21**, 474206 (2009).
- <sup>30</sup>D. C. Joy, M. S. Prasad, and H. M. Meyer, *J. Microsc.-Oxford* **215**, 77 (2004).
- <sup>31</sup>J. Marbach, F. X. Bronold, and H. Fehske, *Phys. Rev. B* **84**, 085443 (2011).
- <sup>32</sup>J. Kroeger, *Rep. Prog. Phys.* **69**, 899 (2006).